Revised phylogeny from complete mitochondrial genomes of phyllostomid bats resolves subfamilial classification

M Alejandra Camacho, Dániel Cadar, Balázs Horváth, Andrés Merino-Viteri, Jérôme Murienne

Abstract

Molecular phylogenies of Phyllostomidae have been classically inferred using a combination of few mitochondrial and nuclear markers; however, there is still uncertainty in the classification, especially among deep clades within the family. In this study, we provide newly sequenced complete mitochondrial genomes from 26 bat species, including 23 species' genomes reported for the first time. By carefully analyzing under Maximum Likelihood and Bayesian methods different ingroup and outgroup samples, partition schemes, and data types, we investigated the robustness and sensitivity of our phylogenetic results. The optimal topologies were those inferred with the complete data matrix of nucleotides, with complex and highly parameterized substitution models and partition schemes. Our results show a statistically robust picture of the evolutionary relationships between phyllostomid subfamilies and clarify hitherto uncertain relationships of Lonchorhininae and Macrotinae.

KEYWORDS: Lonchorhininae - Macrotinae – mitochondrial genomes – phylogenetics Phyllostomidae

INTRODUCTION

The New World leaf-nosed bats, family Phyllostomidae Gray 1825, are found ubiquitously in all regions of the Neotropics. The most recent classification recognizes 227 species in 61 genera (Simmons y Cirranello, 2022), making it the second most speciose chiropteran family after Vespertilionidae Gray 1821. This group of bats is characterized by its rapid early radiation and recent speciation events (Velazco, 2005; Solari *et al.*, 2009; Larsen *et al.*, 2013; Velazco & Patterson, 2013, 2019) that led to an unparalleled morphological, behavioral, and ecological diversity (Freeman, 2000; Dumont *et al.*, 2012; Dávalos *et al.*, 2012; Dávalos *et al.*, 2014; Baker *et al.*, 2016), and an exceptional diversification of feeding habits with six different strategies: sanguivory, insectivory, frugivory, nectivory, carnivory, and omnivory (Baker *et al.* 2012). According to Baker *et al.* (2016), Phyllostomidae is divided into eleven subfamilies, twelve tribes and nine subtribes.

Several phylogenetic studies have examined the relationships among phyllostomid bats using nuclear and mitochondrial loci obtained from classical Sanger sequencing (Baker *et al.*, 2003; Datzmann *et al.*, 2010; Rojas *et al.*, 2011; Dumont *et al.*, 2012; Dávalos *et al.*, 2014; Rojas et al., 2016). Among these studies, Rojas *et al.* (2016) inferred a phylogeny from seven nuclear and five mitochondrial genes, which has been used as a backbone for evolutionary inferences in phyllostomids (Potter *et al.*, 2021). Despite these comprehensive analyses, there is still considerable debate about the position of Lonchorhininae Gray 1866, Micronycterinae Van Den Bussche 1992, and Macrotinae Van Den Bussche 1992, at a deeper level. In addition, further studies are required to solve the systematics of certain groups at the genera level; specially those that have been traditionally underrepresented due to limited

taxonomic sampling, limited data sets, and incongruences among and within different data types, leading to conflicts when drawing taxonomic or systematic conclusions (Solari *et al.*, 2009; Baker *et al.*, 2016; Solari *et al.*, 2019b; Morales-Martínez *et al.,* 2021).

Botero-Castro *et al.* (2013) used high-throughput sequencing to obtain complete mitogenomes through a genome-skimming approach. Using shallow sequencing, this approach is able to fully recover repeated regions of the genome, typically organelles such as the mitochondria (Straub *et al.*, 2012; Trevisan *et al.*, 2019). In their study, Botero-Castro *et al.* (2013) sequenced the complete mitochondrial genome of eleven bat species, including representatives of seven phyllostomid subfamilies, and compared the phylogenies from mitochondrial genomes versus nuclear exons (*rag2* and *vWF*), and single-gene versus concatenation for both kinds of genes. They found that the phylogeny inferred from concatenated mitogenomic sequences was better resolved and well supported. Following their previous study, Botero-Castro *et al.* (2018) sequenced eight new chiropteran mitogenomes and added sequences from GenBank, consolidating a sample of 39 bat species including 19 phyllostomids representing each subfamily as defined by Baker *et al.* (2003).

Complete mitochondrial genomes in vertebrates may provide a better resolution of phylogenetic relationships on various taxonomic levels than short nuclear and mitochondrial fragments classically used with Sanger sequencing data (Meganathan *et al.*, 2012; Finstermeier *et al.*, 2013; Fabre *et al.*, 2017; Botero-Castro *et al.*, 2018; Pan *et al.*, 2020; Hassanin *et al.*, 2020). In addition, advances of high-throughput sequencing technologies in the last decade provide efficient access to mitochondrial

genome sequences (Springer *et al.*, 2004; Paijmans *et al.*, 2013; Morgan *et al.*, 2014; Phillips & Shazwani-Zakaria, 2021; Toussaint *et al.*, 2021).

The seminal work of Botero Castro *et al.* (2013, 2018) provided the foundation for phyllostomids mitochondrial phylogenomics. However, the results are based on a very limited dataset of bats, representing 2.6% of the order's diversity. In this study, using high-throughput sequencing, we have generated several complete bat mitogenomes to reconstruct a subfamily-level phylogeny of phyllostomids. We herein addressed the following questions: (i) does the newly sequenced mitogenomic data help to improve the phylogeny at the subfamily level? (ii) what is the influence of various analytical conditions on the results? In particular, we investigated the influence of partition schemes, choice of outgroups, data type and phylogenetic methods.

MATERIAL AND METHODS

TAXON SAMPLING, DNA EXTRACTION AND SEQUENCING

We newly sequenced 32 mitogenomes from 26 new species out of which 23 belong to Phyllostomidae, two to Vespertilionidae, and one to Molossidae Gervais 1856. The tissues used for DNA extraction belonged to specimens collected in various field trips from western provinces of Ecuador (Figure 1), as part of research projects of the Mammalogy Section of the Museum of Zoology of the Pontifical Catholic University of Ecuador (QCAZ). Additional information about these specimens can be retrieved from https://bioweb.bio/faunaweb/mammaliaweb/. In addition, we used 39 complete mitogenome sequences generated by Botero-Castro *et al.* (2013, 2018), composed of 37 sequences from eight chiropteran and two non-chiropteran

families. Our dataset was thus formed by 71 complete mitogenomes (Table 1). Only three species are represented by two mitogenome sequences: *Desmodus rotundus* Wied-Neuwied, 1826 (Desmodontinae J.A. Wagner, 1840), *Micronycteris megalotis* (Micronycterinae Van Den Bussche, 1992), and *Artibeus lituratus* Leach, 1821.

Bat tissue sections (heart, liver, lungs) were pooled per specimen and introduced in 2 mL safe-lock tubes (Eppendorf, Hamburg, Germany) with tungsten carbide beads (3 mm, Qiagen, Hilden, Germany) and 0.7 mL chilled high-glucose (4.5 g/L) Dulbecco's modified Eagle's medium (DMEM) (Sigma-Aldrich, St. Louis, MO, USA). Bats tissues were homogenized with a TissueLyser II (Qiagen, Hilden, Germany) for 2 min at 30–50 Hz. The suspension was clarified by centrifugation for 1 min at 8000 rpm at 4°C. DNA and RNA were extracted using the MagMAX CORE Nucleic Acid Purification Kit (ThermoFisher Scientific, Waltham, MA, USA) according to manufacturer's recommendations. The quality and quantity of extracted nucleic acids were measured using Qubit™ DNA/RNA HS Assay Kit (Thermo Fisher Scientific, Austin, TX, USA). The extracted DNA (120 ng starting concentration) was subjected to library preparation using a QIAseq FX DNA Library Kit (Qiagen, Hilden, Germany) according to the instructions of the manufacturer. Normalized samples were pooled and sequenced on an Illumina NextSeq550 sequencing platform using the 300-cycle (2 × 150 bp paired-end) NextSeq550 reagent kit (Illumina, San Diego, CA, USA).

MITOGENOME ASSEMBLY AND ANNOTATIONS

The paired-end Illumina reads were quality checked, automatically trimmed, and merged using QIAGEN CLC Genomics Workbench 20.0 (https://digitalinsights.qiagen.com/). Additional adapter trimming and

deduplication was performed using the BBtools software package (https://sourceforge.net/projects/bbmap/). The resulting high-quality reads were *de novo* assembled with Megahit, which in this case was found to give the best output (Li *et al.*, 2015). We used reference guided mapping, circularization validation, manual curation, also using the CLC Genomics Workbench 20.0 software. All the assembled mitochondrial genomes were annotated using MITOS2 metazoan pipeline (Bernt *et al.*, 2013; Al Arab *et al.*, 2017; Donath *et al.*, 2019), followed by manual adjustment in Geneious 9.0.5 (https://www.geneious.com). We relied on the publicly available mitochondrial sequences as reference (Botero-Castro *et al.*, 2013, 2018). In order to validate the morphological identification of the bat species, we used the Barcoding of Life Database Identification Engine on the 5' region of the COI sequence using the BOLD web server (Ratnasingham & Hebert, 2007).

ALIGNMENT AND PHYLOGENY

Ribosomal RNA and transfer RNA loci were aligned using MUSCLE (Edgar, 2004). Sequences of protein-coding genes were aligned using TranslatorX (Abascal *et al.*, 2010) to preserve the reading frame. We used trimAl (Capella-Gutiérrez *et al.*, 2009) to remove poorly aligned regions. Following Botero Castro *et al.* (2018), the protein-coding gene *nd6* and the control region were excluded from the analyses. The *nd6* gene has frequently been omitted because it is coded on the light strand, and its properties differ from those of the other 12 protein-coding genes (Springer *et al.*, 2001; Gao *et al.*, 2018); the control region is the most variable region because of a faster rate of evolution as compared with the rRNA and protein-coding genes of the mitochondrial genome (Gong *et al.*, 2015), which may interfere in the phylogenetic

interpretation. The final data matrix consisted of 71 mitogenomes, each comprising 36 loci (two rRNA, 12 protein-coding and 22 tRNA genes) and averaging 16 kb.

In order to evaluate the impact of ingroup taxon sampling on the results, we performed a phylogenetic analysis using the same analytical parameters and the same outgroups as in Botero-Castro *et al.* (2018), but with an ingroup taxon sampling that significantly exceeds previous analyses. In their study, Botero-Castro *et al.* (2018) used sequences from 19 phyllostomid species while we here used 42 species. We consider this step as our "reference analysis" and the resulting topology as our "reference tree".

To evaluate the influence of partitioning, we analyzed various *a priori* schemes as well as new estimated ones. For the *a priori* nucleotide partition schemes, following Botero-Castro *et al.* (2018), we used one partition, five partitions (two independent partitions for rRNAs and tRNAs combined with three partitions corresponding to each codon position), 14 partitions (two independent partitions for rRNAs and tRNAs plus one partition for each protein-coding gene), and 38 partitions (two independent partitions for rRNAs and for tRNAs plus 36 partitions, one partition for each codon for each gene). For each *a priori* partition scheme, we used a Generalized Time Reversible model of substitution rates along with a Gamma distribution and a fraction of invariable sites (GTR+G+I). In addition, we also estimated the optimal partition scheme and evolutionary model using PartitionFinder 2.1.1 (Lanfear *et al.*, 2012) and ModelFinder (Kalyaanamoorthy *et al.*, 2017) as implemented in IQ-TREE 2 (Minh *et al.*, 2020) (Table 2). The best partitioning schemes were chosen based on the Akaike Information Criterion (AIC) (Bozdogan, 1987).

To evaluate the impact of taxon sampling in the outgroups, we compared our reference analysis from the complete sample of 71 sequences (henceforth "Full outgroup dataset") with a new dataset comprising a subset of 48 nucleotide sequences with only the mitochondrial genomes of Noctilionidae Gray, 1821 and Mormoopidae Saussure, 1860 as outgroups ("Reduced outgroup dataset") (Table 2). We followed Baker *et al.* (2003) who repeatedly found these families as outgroups of Phyllostomidae in their higher-level classification analyses with both mitochondrial and nuclear markers. For each dataset, we estimated the best nucleotide substitution models and partitioning schemes (Table 2).

We also performed various analyses using our dataset as amino acids. We only considered the coding genes and evaluated the impact of outgroups and partitioning schemes as with the nucleotides. For amino acid data sets, we used one and twelve partitions (one for each protein-coding gene) as proposed by Botero-Castro *et al.* (2018), and the resulting best-fit schemes suggested by PartitionFinder and ModelFinder (Table 3). The *a priori* partitions were analyzed with a LG and mtMAM model of substitution rates, respectively, along with a Gamma distribution and a fraction of invariable sites (LG+G+I; mtMAM+G+I). The best partitioning schemes were chosen based on the Akaike Information Criterion (AIC). As with nucleotides, we evaluated the impact of outgroups by comparing our reference analysis (71 mitogenomes with full outgroups) with a dataset comprising a subset of 48 amino acids sequences with only Noctilionidae and Mormoopidae as outgroups.

We performed an additional analysis considering only the coding genes from our full nucleotide dataset using a 36-partition scheme (one partition for each codon for each gene, excluding *nd6*). This analysis was performed to examine the influence of

the data type (amino acid versus the nucleotide) using the exact same dataset (only the protein coding genes).

We performed Maximum Likelihood analyses using RAxML-NG (Kozlov *et al.*, 2019) starting from 10 parsimony trees and 10 random trees. Bootstrapping was performed with the bootstopping option ("bs-trees autoMRE{N}" command). Bootstrap support values were obtained using the classical Felsenstein metric (Felsenstein, 1985) and Transfer Bootstrap Expectation (Lemoine *et al.*, 2018). For comparative reasons, we also inferred the ML tree using IQ-TREE2 (Minh *et al.*, 2020) using the edge-linked partition model (Nguyen *et al.*, 2015; Chernomor *et al.*, 2016) and obtained node support with the ultrafast bootstrap (Hoang *et al.*, 2018) by performing 1000 replicates. Bayesian Inference analyses were performed using MrBayes 3.2.7 (Ronquist *et al.*, 2012). We partitioned the sequences in 38 sets corresponding to two independent partitions for rRNAs and for tRNAs plus 36 partitions, one partition for each codon for each gene, and used the best analytical scheme as evaluated by the Akaike information criterion (AIC). We ran eight MCMC chains for ten million generations with default heating values. The sampling frequency was set every 1000 generations and the first 25,000 samples were discarded as burn-in. A consensus tree was built under the majority rule consensus of all trees obtained in the eight runs after the burn-in period. We used the ''sumt'' command to produce summary statistics for trees sampled during a Bayesian MCMC analysis. Posterior probabilities of nodes were regarded as estimators of confidence. Finally, trees were visualized and edited in FigTree v1.4.4 (http://tree.bio.ed.ac.uk/software/figtree/). Only the optimal partitioning schemes found under ML, were evaluated using Bayesian inference.

RESULTS

After DNA extraction and sequencing, we obtained a mean of 640,043 reads (SD 329,238) per library (Table 4). Among the 32 newly generated mitochondrial genomes, 23 species' genomes have not been published and are first reported here. All mitochondrial genomes show the typical circular structure with an average length of 16,690 pb (SD 152 pb; Table 4) and harbor the gene order found in other mammalian genomes (Pumo *et al.*, 1998; López-Wilchis *et al.*, 2017).

REFERENCE ANALYSIS

We used as reference the phyllostomid phylogeny inferred from all genes under Maximum Likelihood (ML) using RAxML-NG (Kozlov *et al.*, 2019). Sequence evolution was modeled using a GTR+G+I model and a 38-partition scheme comprising two independent partitions for rRNAs and for tRNAs, plus one partition per gene and per codon position for each coding gene. We used 71 complete mitogenomes which included the "Full outgroup dataset" (Table 2). In essence, this analysis corresponds exactly to the one previously performed by Botero-Castro *et al.* (2018) except for the ingroup where we added 23 new phyllostomid species to the 19 previously used in 2018. As expected, Phyllostomidae is recovered as monophyletic and divided into eleven clades corresponding to all known subfamilies (Figure 1). At the level of deep nodes (subfamilies), we cannot observe differences between our reference topology and the best evaluated topology obtained by Botero-Castro *et al.* (2018), however, the addition of new mitogenomes shows genus-level relationships not presented by Botero-Castro *et al.* (2018) that help clarify the relationships between species, particularly those in nectar-feeding

subfamilies. When compared with the other analyses that combine mitochondrial and nuclear markers (Baker, 2000; Baker *et al.*, 2003; Rojas *et al.*, 2016), the main difference in our analysis lies in the position of Lonchorhininae as sister group to Phyllostominae Gray, 1825, not to a clade formed by Lonchophyllinae Griffiths, 1982 and the mainly frugivore subfamilies.

The phylogenetic relationships between the Stenodermatinae Gervais, 1856, Rhinophyllinae Baker, Solari, Cirranello & Simmons, 2016, Carolliinae and Glyphonycterinae Baker, Solari, Cirranello & Simmons, 2016 subfamilies are recovered with strong support. Stenodermatinae shares a common ancestry with Rhinophyllinae after diverging from a clade formed by Carolliinae and Glyphonycterinae. Regarding the nectar-feeding phyllostomids, Lonchophyllinae appears as sister to a lineage comprising the clades formed by Stenodermatinae + Rhinophyllinae and Carolliinae + Glyphonycterinae (Figure 2), with a strong nodal support (BS=91%, node not recovered with Bayesian inference) and in agreement with Baker *et al.* (2003), Rojas *et al.* (2011), and Rojas *et al.* (2016). Glossophaginae Bonaparte, 1845 is the nectar-feeding clade that diverged first and is composed of two major lineages: one containing *Anoura* Gray, 1838 and *Choeroniscus*, and the other containing *Glossophaga* E. Geoffroyi, 1818 and *Brachypylla* Gray, 1833. In addition, Phyllostominae appears as a sister group to Lonchorhininae with moderate bootstrap support and vampire bats are defined as a three-genus monophyletic clade (Desmodontinae), with well-resolved relationships. In our reference tree, Macrotinae is recovered as sister group to all remaining Phyllostomid subfamilies, and Mormoopidae appears as sister family to Phyllostomidae, also in concordance with previous phylogenetic reconstructions

(Baker *et al.*, 2003, 2016; Cirranello *et al.*, 2016). All phylogenetic relationships between non-Phyllostomid families remained consistent with the results obtained in previous studies with mitogenomes except that, for the first time, mitogenomes of the family Molossidae (*Molossus molossus* É. Geoffroy, 1805) are added and appear closely related to Vespertilionidae.

IMPACT OF PARTITIONING SCHEMES

We performed twelve different analyses with various *a priori* partition schemes as well as new estimated ones (Table 2). We did find that a GTR+G+I evolution model along with a 38-partitions scheme (thus corresponding to our "Reference analysis") yielded the smallest AIC value (Table 2). This evolutionary model and partition scheme also yielded the best AIC value in the analysis performed by Botero-Castro *et al.* (2018). The eleven additional analytical schemes are thus sub-optimal in the sense that they yielded higher AIC values than with the optimal partitioning scheme, including those with IQ-TREE2 performed for comparative reasons. This evaluation is however particularly relevant as it provides a different view of the stability of our results compared to statistical resampling like bootstrap. The presence (or not) of key clades was thus evaluated with a sensitivity analysis of the various analytical conditions and is represented with a Navajo rug approach (Figure 2).

Across the analyses, we were able to identify very stable nodes. The phylogenetic relationships between the Stenodermatinae, Rhinophyllinae, Carolliinae and Glyphonycterinae subfamilies are recovered in all the analyses. Rhinophyllinae appears consistently as a sister clade to Stenodermatinae and both subfamilies form a sister clade to another formed by Carolliinae and Glyphonycterinae. Vampire bats (Desmodontinae) consistently appear in the same position in all the resulting

topologies, and the relationships between the three species were all well resolved. Interestingly, the subfamily Lonchorhininae whose position was poorly supported in previous studies (Rojas *et al.*, 2016) is very stable as sister to Phyllostominae in our analyses.

We identified unstable nodes formed by subfamilies whose phylogenetic relationships varied depending on the number of partitions. Lonchophyllinae as sister to the clade formed by Stenodermatinae + Rhinophyllinae and Carolliinae + Glyphonycterinae appear in only four out of the twelve analyses with bootstraps values ranging from 63% to 96%. Lonchophyllinae is found as sister to a clade comprised by Lonchorhininae, Phyllostominae, Glossophaginae, Glyphonycterinae, Carolliinae, Rhinophyllinae and Stenodermatinae, depicting even better bootstrap values in the corresponding analyses (BS = 91%–100%). The subfamily is also recovered as sister to Glossophaginae in several analytical schemes, with medium to strong support values (BS = 45%–97%). As the position of Lonchophyllinae change in the topologies, so does Glossophaginae and its phylogenetic placement. Macrotinae appears as a sister group of all remaining phyllostomids in fifty percent of the analyses performed, with absolute support (BS = 100%, PP = 1); however, Micronycterinae is also recovered as sister clade to all remaining phyllostomids (including Macrotinae) in the other fifty percent of the analyses, also with very high support (BS = 100%; PP = 1).

IMPACT OF OUTGROUPS TAXON SAMPLING

By comparing the topologies obtained with the “Full outgroup dataset” and the “Reduced outgroup dataset” (Table 2) we observe an effect caused by the number of outgroups used. Although most of the phylogenetic relationships using less

outgroups are consistent with the reference tree obtained from the analysis of 71 sequences, some relationships are less stable. In most of the analyses with the "Full outgroup dataset", Lonchophyllinae appears as sister to the nodes formed by Stenodermatinae + Rhinophyllinae and Carolliinae + Glyphonycterinae; however, in almost all the analyses performed with the "Reduced outgroup dataset", Lonchophyllinae is recovered as sister to Glossophaginae, with medium to strong support values (BS = 45%–97%). Taking this parameter into account, here again, we observe that as the position of Lonchophyllinae changes in the topologies, so does Glossophaginae and its phylogenetic placement. Unlike what was observed in all the analyses with all the sequences, with the "Reduced outgroup dataset", we found Micronycterinae as sister clade to all remaining phyllostomids (including Macrotinae; BS = 75%–89 %), although less supported than Macrotinae as the sister clade to all remaining phyllostomids found with the "Full outgroup dataset".

IMPACT OF DATA TYPE

The phylogenetic resolution and associated nodal supports across analyses differ significantly according to the type of data (i.e., nucleotides vs. amino acids). For amino acids, we performed eight different analyses (Table 3). All resulting topologies were compared, and the presence (or not) of key clades is represented with a Navajo rug approach as well (Figure S1). For amino acid data sets, the best-evaluated topology is poorly supported and does not agree with the best-evaluated topology of the nucleotide analyses.

Phyllostomidae is recovered as monophyletic and divided into eleven clades corresponding to all known subfamilies; however, as a generality, we also found

more unstable nodes with lower support than with nucleotides. We found Lonchophyllinae as sister to a clade comprised of Lonchorhininae, Phyllostominae, Glossophaginae, Glyphonycterinae, Carolliinae, Rhinophyllinae, and Stenodermatinae with strong bootstrap supports (BS = 98%, node not recovered with Bayesian inference) (Figure S1); also, we found Lonchophyllinae as the nectar-feeding clade that diverged first and as sister to a clade containing Glossophaginae which then diverged from a lineage containing Glyphonycterinae, Carollinae, Rhinophyllinae and Stenodermatinae, with poor to strong support values (BS = 40%–91%). Finally, we found Lonchophyllinae forming a monophyletic clade with Glossophaginae. The position of Lonchorhininae appears unclear when amino acid data sets were analyzed. As with nucleotides, we found Lonchorhininae as sister to Phyllostominae in some analyses although mostly with poor bootstrap support. In most of the amino acid analyses, Lonchorhininae appears as sister to clades containing the subfamilies Phyllostominae, Lonchophyllinae, Glossophaginae, Glyphonycterinae, Carolliinae, Rhinophyllinae, and Stenodermatinae. Another important variation in relation to the results we obtained with nucleotide data sets was the position of Micronycterinae: in all the analysis carried out with amino acids Micronycterinae appears as the sister lineage to all the other phyllostomids with strong support values (BS = 90%–100%). Our analysis considering only the coding genes from our full nucleotide dataset using a 36-partition scheme yielded a topology that mostly resembled the best-evaluated phylogeny from the amino acid data set and also does not agree with the best-evaluated topology of the nucleotide analyses (Figure S2).

IMPACT OF PHYLOGENETIC METHODS

For the Bayesian inference, we used the same analytical scheme as for Maximum Likelihood. We observe that the phylogenetic resolution and associated nodal supports differ depending on the inference method. Even with high bootstrap values, some nodes are not recovered under Bayesian Inference. Figure 2 (for nucleotides) and S1 (for amino acids) summarize and compare the support values of the ML analyses and the BI posterior probabilities with a pattern of colored semicircles. In the trees, it can be observed that the absence of a semicircle represents the non-recovery of a particular node by ML or BI.

Under Bayesian Inference we observe relationships between subfamilies (particularly in the less stable nodes) statistically less likely to occur due to posterior probabilities lower than 0.5, for example a monophyletic relationship between Lonchophyllinae and Phyllostominae (PP = 0.47). Additionally, the relationships between Lonchorhininae with the rest of the subfamilies or those of Micronycterinae or Macrotinae as basal clades of Phyllostomidae are neither clear nor consistent under Bayesian analysis.

DISCUSSION

In this study, we provide newly sequenced complete mitogenomes for 26 bat species, from 16 genera, and three families. Our phylogenomic analysis of phylostomids confirmed the relationships so far agreed between the subfamilies, with strong supports and highly congruent with those previously suggested by Baker *et al.* (2016), Rojas *et al.* (2016), and Botero-Castro *et al.* (2018). Phyllostomidae was monophyletic and divided into eleven subfamilies. The

phylogenetic relationships between Stenodermatinae, Rhinophyllinae, Carolliinae, and Glyphonycterinae, as well as the position of Desmodontinae were consistent and well supported. Lonchophyllinae evolved independently of Glossophaginae, although inconsistent results across different analyses were evident among nectar-eating subfamilies (see specific discussion hereafter). Unlike what was found by Rojas *et al.* (2016), Lonchorhininae appears consistently as the sister of Phyllostominae. Finally, in our reference tree, Macrotinae is retrieved as a sister group to all the remaining Phyllostomid subfamilies. Despite high support values both in the ML and BI analyses, our sensitivity analysis highlighted that some relationships were unstable when parameters related to the number of outgroup taxa, number of partitions, and data type (i.e., nucleotides *vs*. amino acids) were evaluated and we hereafter further discuss the stability of our results and their implication for evolutionary studies.

The choice of outgroup could have important consequences for the resulting phylogenetic tree (Graybeal, 1998; Schneider & Cannarozzi, 2009). From all possible outgroups, the closest one is the best choice to root a tree because shorter distances suffer less from statistical error and the expected number of homoplasies between any ingroup and the outgroup is minimized (Muse & Weir, 1992; Smith, 1994). We expected that by removing all other mammalian families and keeping the closest outgroups (Reduced outgroup dataset), the phylogeny of Phyllostomidae could be improved or at least would not be affected. On the contrary, our results showed discrepancy between phylogenies obtained with the full outgroup dataset and the reduced outgroup dataset. We found stronger phylogenetic congruence when all sequences, even those less phylogenetically related, were maintained as outgroups.

This is particularly true for the most basal nodes in phyllostomids, related to the phylogenetic placement of Macrotinae and Micronycterinae.

Early debates concentrated on the choice of the appropriate evolutionary model (Kelsey *et al.*, 1999), with the adequacy of the model potentially producing differences between topologies with short internal branches (Schneider & Cannarozzi, 2009). However, it is now well recognized that choosing the most adequate model is unimportant and that using the most complex model provides consistent topologies (Abadi *et al.*, 2019). However, variation in substitution patterns across genes and sites should still be accommodated and the partitioning of the dataset can have strong influence on the topology (Kainer & Lanfear, 2015). Likewise, some of our results proved to be sensitive to the choice of the partitioning scheme. This is particularly visible in the "intermediate" part of the tree (between the shallowest nodes and the deeper nodes) where branch lengths are noticeably shorts. The optimal results are however quite stable as they are retrieved in four out six partition schemes.

Of all the analytical schemes that we evaluated, a strong influence of the data type (nucleotides *vs* amino acids) has been observed. In general, the best-evaluated model for amino acids yielded a topology that was incongruent with the best-evaluated nucleotide topology. Our most well-supported result for amino acids (71 samples with a 7–partition scheme; Figure S1) contradicts most previous relevant molecular analyses (Baker, 2000; Baker *et al.*, 2003; Rojas *et al.*, 2011, 2016; Dávalos *et al.*, 2012; Cirranello *et al.*, 2016), although it is congruent with the best evaluated topology for amino acids by Botero-Castro *et al.* (2018). Both ML and BI analyses reconstructed a similar topology; however, more key clades showed lower support

values, if compared to nucleotides data sets. These low phylogenetic resolutions may be due to the use of coding genes only and thus fewer characters. This was demonstrated with the analysis we did using only coding genes from the nucleotide data set (Figure S2).

In our reference tree, Lonchophyllinae and Glossophaginae were not sister clades. Both ML and BI analyses strongly support the non-monophyly of these lineages. However, the most notorious incongruities across analyses were those related to the phylogenetic position of the nectar-eating subfamilies. In the case of nectarivores, five out of twelve analyses carried out with nucleotides and one out of eight analyses carried out with amino acids, depicted these two subfamilies as monophyletic. Although these results may agree with morphological phylogenies such as Wetterer *et al.*'s (2000) and some of the analyses made by Dávalos *et al.* (2012), our best-supported results showed both groups as not sister taxa. The homoplasies observed in the aforementioned morphological phylogenies may be the result of morphological similarities associated with ecological adaptations to nectar feeding (Gatesy *et al.*, 1996; Sánchez-Villagra & Williams, 1998; Wiens *et al.*, 2003). However, profound examination of morphological characters such as the oral muscle complexes (Griffiths, 1982; Datzmann *et al.*, 2010) and recent extensive molecular analyses (Baker *et al.*, 2016; Rojas *et al.*, 2016) strongly support that Lonchophyllinae and Glossophaginae evolved nectarivory independently, a result confirmed by our analyses.

Across most of our analyses, the position of Lonchorhininae is stable and well supported as sister to Phyllostominae. Until the beginning of this century, *Lonchorhina* was placed within Phyllostominae (Baker *et al.*, 1989; Koopman, 1994;

Wetterer *et al.*, 2000; Jones *et al.*, 2002). Baker *et al.* (2003) included *Lonchorhina* Tomes, 1863 within its own monogeneric subfamily, Lonchorhininae, using as evidence a Bayesian analysis that combined the nuclear gene *rag2*, the mitochondrial genes 12S rRNA, Val tRNA, and 16S rRNA. In this analysis, *Lonchorhina* diverged from the remainder of the phyllostomids after the divergence of vampires but before the common ancestor of the remaining subfamilies. Rojas *et al.* (2011), analyzed the same genes as Baker *et al.* (2003), although it resulted in another hypothesis in which *Lonchorhina* appeared as sister to a clade comprising Glossophaginae, Lonchophyllinae, Carolliinae, Glyphonycterinae, Rhinophyllinae and Stenodermatinae. Later, Rojas *et al.* (2016) in a comprehensive phylogenetic analysis using combinations of seven nuclear loci and five mitochondrial genes from phyllostomid species found *Lonchorhina* as sister to a clade that excluded Glossophaginae and Phyllostominae, although with poor support (i.e., bootstrap value < 50%). Our phylogenomic approach supports Lonchorhininae as a sister to Phyllostominae. We herein provide a better resolution of the phylogenetic relationships between these insectivore subfamilies; although we consider that this hypothesis could be evaluated by analyzing molecular data from all species in the genus. The six species included in *Lonchorhina* are essentially insectivores and are characterized by having highly developed and quite complex ears, tragi, and nasal leaves (Solari *et al.*, 2019a). Representatives of *Lonchorhina* depend on caves for roosting, which are, in general, difficult to access causing specimens to be very rare in museum collections (Mantilla-Meluk & Montenegro, 2016). The incomplete taxonomic coverage, both morphological and molecular, has historically prevented an accurate reconstruction of the relationships within *Lonchorhina* and among Lonchorhininae and other subfamilies.

CONCLUSION

Our mitogenomic analysis yielded a topology that was well supported and highly congruent with previous phylogenetic results. Despite variations across analyses, our optimal topology confirmed the known relationships among most subfamilies, nectarivores evolved independently, and Macrotinae is sister to all other subfamilies. We also propose the hypothesis that Lonchorhininae may be the sister subfamily of Phyllostominae. We found that deeper relationships were sensible to the outgroup and data type selection, and that the intermediate relationships characterized by short internal branches were sensible to the partitioning schemes. Under adequate analytical conditions, complete mitogenomes proved to be extremely useful for resolving patterns of phylogenetic relationships within phyllostomids. This is of particular interest considering that genome-skimming is probably the most efficient method to analyze museum specimens or highly degraded material, which in turn may be the only accessible evidence for solving taxonomic conundra. In addition, future improvements on the phylogeny of phyllostomid could come from inclusion of more species and the use of large nuclear datasets such as transcriptomics, gene capture or full genome sequencing (Tsagkogeorga *et al.*, 2013; Lei & Dong, 2016; McCormack *et al.*, 2016 2016; Potter *et al.*, 2021).

ACKNOWLEDGEMENTS

REFERENCES

Abadi S, Azouri D, Pupko T, Mayrose I. 2019. Model selection may not be a mandatory step for phylogeny reconstruction, *Nature Communications* 10: 934.

Abascal F, Zardoya R, Telford MJ. 2010. TranslatorX: multiple alignment of nucleotide sequences guided by amino acid translations, *Nucleic Acids Research* 38: W7–13.

Al Arab M, Höner Zu Siederdissen C, Tout K, Sahyoun AH, Stadler PF, Bernt M. 2017. Accurate annotation of protein-coding genes in mitochondrial genomes, *Molecular Phylogenetics and Evolution* 106: 209–216.

Baker RJ, Porter CA, Patton JC, Van Den Bussche RA. 2000. Systematics of bats of the family Phyllostomidae based on RAG2 DNA sequences, *Occasional Papers, The Museum, Texas Tech University*, 201:1–16.

Baker RJ, Bininda-Emonds ORP, Mantilla-Meluk H, Porter CA, Van Den Bussche RA. 2012. Molecular timescale of diversification of feeding strategy and morphology in New World Leaf-Nosed Bats (Phyllostomidae): a phylogenetic perspective. In: Gunnell GF, Simmons NB, eds. *Evolutionary history of bats: fossils, molecules and morphology*. Cambridge: Cambridge University Press, 385–409.

Baker RJ, Hood CS, Honeycutt RL. 1989. Phylogenetic Relationships and Classification of the Higher Categories of the New World Bat Family Phyllostomidae, *Systematic Biology* 38: 228–238.

Baker RJ, Hoofer SR, Porter CA, Van Den Bussche RA. 2003. Diversification among New World leaf-nosed bats: an evolutionary hypothesis and classification inferred from digenomic congruence of DNA sequence, *Occasional Papers, Museum of Texas*

Tech University 230: 1–32.

Baker RJ, Solari S, Cirranello A, Simmons NB. 2016. Higher level classification of phyllostomid bats with a summary of DNA synapomorphies, *Acta chiropterologica / Museum and Institute of Zoology, Polish Academy of Sciences* 18: 1–38.

Bernt M, Donath A, Jühling F, Externbrink F, Florentz C, Fritzsch G, Pütz J, Middendorf M, Stadler PF. 2013. MITOS: improved de novo metazoan mitochondrial genome annotation, *Molecular Phylogenetics and Evolution* 69: 313–319.

Botero-Castro F, Tilak MK, Justy F, Catzeflis F, Delsuc F, Douzery EJP. 2013. Next-generation sequencing and phylogenetic signal of complete mitochondrial genomes for resolving the evolutionary history of leaf-nosed bats (Phyllostomidae), *Molecular Phylogenetics and Evolution* 69: 728–739.

Botero-Castro F, Tilak MK, Justy F, Catzeflis F, Delsuc F, Douzery EJP. 2018. In Cold Blood: Compositional Bias and Positive Selection Drive the High Evolutionary Rate of Vampire Bats Mitochondrial Genomes, *Genome Biology and Evolution* 10: 2218–2239.

Bozdogan H. 1987. Model selection and Akaike's Information Criterion (AIC): The general theory and its analytical extensions, *Psychometrika* 52: 345–370.

Capella-Gutiérrez S, Silla-Martínez JM, Gabaldón T. 2009. trimAl: a tool for automated alignment trimming in large-scale phylogenetic analyses, *Bioinformatics* 25: 1972–1973.

Chernomor O, von Haeseler A, Minh BQ. 2016. Terrace Aware Data Structure for

Phylogenomic Inference from Supermatrices, *Systematic Biology* 65: 997–1008.

Cirranello A, Simmons NB, Solari S, Baker RJ. 2016. Morphological diagnoses of higher-level phyllostomid taxa (Chiroptera: Phyllostomidae), *Acta chiropterologica / Museum and Institute of Zoology, Polish Academy of Sciences* 18: 39–71.

Datzmann T, von Helversen O, Mayer F. 2010. Evolution of nectarivory in phyllostomid bats (Phyllostomidae Gray, 1825, Chiroptera: Mammalia), *BMC Evolutionary Biology* 10: 165.

Dávalos LM, Cirranello AL, Geisler JH, Simmons NB. 2012. Understanding phylogenetic incongruence: lessons from phyllostomid bats, *Biological reviews of the Cambridge Philosophical Society* 87: 991–1024.

Dávalos LM, Velazco PM, Warsi OM, Smits PD, Simmons NB 2014. Integrating incomplete fossils by isolating conflicting signal in saturated and non-independent morphological characters, *Systematic Biology* 63(4): 582–600

Donath A, Jühling F, Al-Arab M, Bernhart SH, Reinhardt F, Stadler PF, Middendorf M, Bernt M. 2019. Improved annotation of protein-coding genes boundaries in metazoan mitochondrial genomes, *Nucleic Acids Research* 47: 10543–10552.

Dumont ER, Dávalos LM, Goldberg A, Santana SE, Rex K, Voigt CC. 2012. Morphological innovation, diversification, and invasion of a new adaptive zone, *Proceedings of the Royal Society B: Biological Sciences* 279: 1797–1805.

Edgar RC. 2004. MUSCLE: a multiple sequence alignment method with reduced time and space complexity, *BMC Bioinformatics* 5: 1-19.

Fabre PH, Upham NS, Emmons LH, Justy F, Leite YLR, Carolina Loss A, Orlando L,

Tilak MK, Patterson BD, Douzery EJP. 2017. Mitogenomic Phylogeny, Diversification, and Biogeography of South American Spiny Rats, *Molecular Biology and Evolution* 34: 613–633.

Felsenstein J. 1985. Confidence limits on phylogenies: an approach using the bootstrap, *Evolution* 39: 783–791.

Finstermeier K, Zinner D, Brameier M, Meyer M, Kreuz E, Hofreiter M, Roos C. 2013. A mitogenomic phylogeny of living primates, *PLoS ONE* 8: e69504.

Freeman PW. 2000. Macroevolution in Microchiroptera: Recoupling morphology and ecology with phylogeny, *Evolutionary Ecology Research* 2: 317–335

Gao S, Chen JJ, Jiang GF. 2018. Complete mitochondrial genome of bamboo grasshopper, *Ceracris fasciata*, and the phylogenetic analyses and divergence time estimation of Caelifera (Orthoptera), *Bulletin of entomological research* 108(3): 321–336.

Gatesy J, Hayashi C, Cronin MA, Arctander P. 1996. Evidence from milk casein genes that cetaceans are close relatives of hippopotamid artiodactyls, *Molecular Biology and Evolution* 13: 954–963.

Graybeal A. 1998. Is it better to add taxa or characters to a difficult phylogenetic problem?, *Systematic Biology* 47: 9–17.

Gong L, Shi W, Si LZ, Wang ZM, Kong, XY. 2015. The complete mitochondrial genome of peacock sole *Pardachirus pavoninus* (Pleuronectiformes: Soleidae) and comparative analysis of the control region among 13 soles, *Molecular Biology* 49(3): 408–417.

Griffiths TA. 1982. Systematics of the New World Nectar-Feeding Bats (Mammalia, Phyllostomidae), Based on the Morphology of the Hyoid and Lingual Regions, *American Museum Novitates* 2742: 1–33.

Hassanin A, Bonillo C, Tshikung D, Pongombo Shongo C, Pourrut X, Kadjo B, Nakouné E, Tu VT, Prié V, Goodman SM. 2020. Phylogeny of African fruit bats (Chiroptera, Pteropodidae) based on complete mitochondrial genomes, *Journal of Zoological Systematics and Evolutionary Research* 58: 1395–1410.

Hoang DT, Chernomor O, von Haeseler A, Minh BQ, Vinh LS. 2018. UFBoot2: Improving the Ultrafast Bootstrap Approximation, *Molecular Biology and Evolution* 35: 518–522.

Jones KE, Purvis A, MacLarnon A, Bininda-Emonds ORP, Simmons NB. 2002. A phylogenetic supertree of the bats (Mammalia: Chiroptera), *Biological Reviews of the Cambridge Philosophical Society* 77: 223–259.

Kainer D, Lanfear R. 2015. The effects of partitioning on phylogenetic inference, *Molecular Biology and Evolution* 32: 1611–1627.

Kalyaanamoorthy S, Minh BQ, Wong TKF, von Haeseler A, Jermiin LS. 2017. ModelFinder: fast model selection for accurate phylogenetic estimates, *Nature Methods* 14: 587–589.

Kelsey CR, Crandall KA, Voevodin AF. 1999. Different models, different trees: the geographic origin of PTLV-I, *Molecular Phylogenetics and Evolution* 13: 336–347.

Koopman KF. 1994. *Chiroptera: Systematics*, Handbook of Zoology. Walter de Gruyter Press, 1–217.

Kim YM, Choi, EH, Kim SK, Jang KH, Ryu SH, Hwang UW 2011. Complete mitochondrial genome of the Hodgson's bat *Myotis formosus* (Mammalia, Chiroptera, Vespertilionidae), *Mitochondrial DNA* 22(4): 71–73.

Kim KS, Lee SE, Jeong HW, Ha JH. 1998. The complete nucleotide sequence of the domestic dog (*Canis familiaris*) mitochondrial genome, *Molecular phylogenetics and evolution* 10(2): 210–220.

Kozlov AM, Darriba D, Flouri T, Morel B, Stamatakis A. 2019. RAxML-NG: a fast, scalable and user-friendly tool for maximum likelihood phylogenetic inference, *Bioinformatics* 35: 4453–4455.

Lanfear R, Calcott B, Ho SYW, Guindon S. 2012. Partitionfinder: combined selection of partitioning schemes and substitution models for phylogenetic analyses, *Molecular biology and evolution* 29: 1695–1701.

Larsen PA, Marchán-Rivadeneira MR, Baker RJ. 2013. Speciation Dynamics of the Fruit-Eating Bats (Genus *Artibeus*): With Evidence of Ecological Divergence in Central American Populations. In: Adams RA, Pedersen SC, eds. *Bat Evolution, Ecology, and Conservation*. New York: Springer, 315–339.

Lei M, Dong D. 2016. Phylogenomic analyses of bat subordinal relationships based on transcriptome data, *Scientific Reports* 6: 27726.

Lemoine F, Domelevo-Entfellner JB, Wilkinson E, Correia D, Dávila Felipe M, De Oliveira T, Gascuel O. 2018. Renewing Felsenstein's Phylogenetic Bootstrap in the Era of Big Data, *Nature* 556: 452–456.

Li D, Liu CM, Luo R, Sadakane K, Lam TW. 2015. MEGAHIT: an ultra-fast single-

node solution for large and complex metagenomics assembly via succinct de Bruijn graph, *Bioinformatics* 31: 1674–1676.

Lin YH, McLenachan PA, Gore AR, Phillips MJ, Ota R, Hendy MD, Penny D. 2002. Four new mitochondrial genomes and the increased stability of evolutionary trees of mammals from improved taxon sampling, *Molecular Biology and Evolution* 19(12): 2060–2070.

Lin YH, Penny D. 2001. Implications for bat evolution from two new complete mitochondrial genomes, *Molecular Biology and Evolution* 18(4): 684–688.

López-Wilchis R, Del Río-Portilla MÁ, Guevara-Chumacero LM. 2017. Mitochondrial genome of *Pteronotus personatus* (Chiroptera: Mormoopidae): comparison with selected bats and phylogenetic considerations, *Genetica* 145: 27–35.

Mantilla-Meluk H, Montenegro O. 2016. Nueva especie de *Lonchorhina* (Chiroptera: Phyllostomidae) de Chiribiquete, Guayana colombiana, *Revista Biodiversidad Neotropical* 6: 171.

McCormack JE, Tsai WLE, Faircloth BC. 2016. Sequence capture of ultraconserved elements from bird museum specimens, *Molecular Ecology Resources* 16: 1189–1203.

Meganathan PR, Pagan HJT, McCulloch ES, Stevens RD, Ray DA. 2012. Complete mitochondrial genome sequences of three bats species and whole genome mitochondrial analyses reveal patterns of codon bias and lend support to a basal split in Chiroptera, *Gene* 492: 121–129.

Minh BQ, Schmidt HA, Chernomor O, Schrempf D, Woodhams MD, von Haeseler A,

Lanfear R. 2020. IQ-TREE 2: New Models and Efficient Methods for Phylogenetic Inference in the Genomic Era, *Molecular biology and evolution* 37: 1530–1534.

Morales-Martínez DM, López-Arévalo HF, Vargas-Ramírez M. 2021. Beginning the quest: phylogenetic hypothesis and identification of evolutionary lineages in bats of the genus *Micronycteris* (Chiroptera, Phyllostomidae), *ZooKeys* 1028: 135–159.

Morgan CC, Creevey CJ, O'Connell MJ. 2014. Mitochondrial data are not suitable for resolving placental mammal phylogeny, *Mammalian genome:* 25: 636–647.

Muse SV, Weir BS. 1992. Testing for equality of evolutionary rates, *Genetics* 132: 269–276.

Nguyen LT, Schmidt HA, von Haeseler A, Minh BQ. 2015. IQ-TREE: a fast and effective stochastic algorithm for estimating maximum-likelihood phylogenies, *Molecular biology and evolution* 32: 268–274.

Nikaido M, Harada M, Cao Y, Hasegawa M, Okada N. 2000. Monophyletic origin of the order Chiroptera and its phylogenetic position among Mammalia, as inferred from the complete sequence of the mitochondrial DNA of a Japanese megabat, the Ryukyu flying fox (*Pteropus dasymallus*), *Journal of Molecular Evolution* 51(4): 318–328.

Nikaido M, Kawai K, Cao Y, Harada M, Tomita S, Okada N, Hasegawa M. 2001. Maximum likelihood analysis of the complete mitochondrial genomes of eutherians and a reevaluation of the phylogeny of bats and insectivores, *Journal of Molecular Evolution* 53(4): 508–516.

Paijmans JLA, Gilbert MTP, Hofreiter M. 2013. Mitogenomic analyses from ancient

DNA, *Molecular phylogenetics and evolution* 69: 404–416.

Pan T, Miao JS, Zhang HB, Yan P, Lee PS, Jiang XY, Ouyang JH, Deng YP, Zhang BW, Wu XB. 2020. Near-complete phylogeny of extant Crocodylia (Reptilia) using mitogenome-based data, *Zoological Journal of the Linnean Society* 191: 1075–1089.

Phillips MJ, Shazwani-Zakaria S. 2021. Enhancing mitogenomic phylogeny and resolving the relationships of extinct megafaunal placental mammals, *Molecular Phylogenetics and Evolution* 158: 107082.

Potter JHT, Davies KTJ, Yohe LR, Sanchez MKR, Rengifo EM, Struebig M, Warren K, Tsagkogeorga G, Lim BK, Dos Reis M, Dávalos LM, Rossiter SJ. 2021. Dietary Diversification and Specialization in Neotropical Bats Facilitated by Early Molecular Evolution, *Molecular Biology and Evolution* 38: 3864–3883.

Pumo DE, Finamore PS, Franek WR, Phillips CJ, Tarzami S, Balzarano D. 1998. Complete mitochondrial genome of a neotropical fruit bat, *Artibeus jamaicensis*, and a new hypothesis of the relationships of bats to other eutherian mammals, *Journal of Molecular Evolution* 47: 709–717.

Ratnasingham S, Hebert PDN. 2007. BOLD: The Barcode of Life Data System (http://www.barcodinglife.org), *Molecular Ecology Notes* 7: 355–364.

Rojas D, Vale A, Ferrero V, Navarro L. 2011. When did plants become important to leaf-nosed bats? Diversification of feeding habits in the family Phyllostomidae, *Molecular Ecology* 20: 2217–2228.

Rojas D, Warsi OM, Dávalos LM. 2016. Bats (Chiroptera: Noctilionoidea) Challenge a Recent Origin of Extant Neotropical Diversity, *Systematic Biology* 65: 432–448.

Ronquist F, Teslenko M, van der Mark P, Ayres DL, Darling A, Höhna S, Larget B, Liu L, Suchard MA, Huelsenbeck JP. 2012. MrBayes 3.2: efficient Bayesian phylogenetic inference and model choice across a large model space, *Systematic Biology* 61: 539–542.

Sánchez-Villagra MR, Williams BA. 1998. Levels of Homoplasy in the Evolution of the Mammalian Skeleton, *Journal of Mammalian Evolution* 5: 113–126.

Schneider A, Cannarozzi GM. 2009. Support patterns from different outgroups provide a strong phylogenetic signal, Molecular Biology and Evolution 26: 1259–1272.

Simmons NB, Cirranello AL. 2022. Bat Species of the World: A taxonomic and geographic database. url: https://batnames.org/ Accessed on 04/06/2022.

Smith AB. 1994. Rooting molecular trees: problems and strategies, *Biological Journal of the Linnean Society* 51: 279–292.

Solari S, Hoofer SR, Larsen PA, Brown AD, Bull RJ, Guerrero JA, Ortega J, Carrera JP, Bradley RD, Baker RJ. 2009. Operational criteria for genetically defined species: analysis of the diversification of the small fruit-eating bats, Dermanura (Phyllostomidae: Stenodermatinae), *Acta chiropterologica / Museum and Institute of Zoology, Polish Academy of Sciences* 11: 279–288.

Solari S, Medellín RA, Rodríguez-Herrera B, Dumont ER, Burneo SF. 2019a. Family Phyllostomidae. In: Wilson DE, Mittermeier RA, eds. *Handbook of the Mammals of the World*. Barcelona: Lynx Ediciones, 444–583.

Solari S, Sotero-Caio CG, Baker RJ. 2019b. Advances in systematics of bats: towards

a consensus on species delimitation and classifications through integrative taxonomy, *Journal of mammalogy* 100: 838–851.

Springer MS, DeBry RW, Douady C, Amrine HM, Madsen O, de Jong WW, Stanhope MJ. 2001. Mitochondrial versus nuclear gene sequences in deep-level mammalian phylogeny reconstruction, *Molecular Biology Evolution* 18: 132–143.

Springer MS, Stanhope MJ, Madsen O, de Jong WW. 2004. Molecules consolidate the placental mammal tree, *Trends in Ecology & Evolution* 19: 430–438.

Straub SCK, Parks M, Weitemier K, Fishbein M, Cronn RC, Liston A. 2012. Navigating the tip of the genomic iceberg: Next-generation sequencing for plant systematics, *American Journal of Botany* 99: 349–364.

Toussaint EFA, Gauthier J, Bilat J, Gillett CPDT, Gough HM, Lundkvist H, Blanc M, Muñoz-Ramírez CP, Alvarez N. 2021. HyRAD-X Exome Capture Museomics Unravels Giant Ground Beetle Evolution, *Genome Biology and Evolution* 13.

Trevisan B, Alcantara DMC, Machado DJ, Marques FPL, Lahr DJG. 2019. Genome skimming is a low-cost and robust strategy to assemble complete mitochondrial genomes from ethanol preserved specimens in biodiversity studies, *PeerJ* 7: e7543.

Tsagkogeorga G, Parker J, Stupka E, Cotton JA, Rossiter SJ. 2013. Phylogenomic analyses elucidate the evolutionary relationships of bats, *Current biology: CB* 23: 2262–2267.

Velazco PM. 2005. Morphological Phylogeny of the Bat Genus *Platyrrhinus* Saussure, 1860 (Chiroptera: Phyllostomidae) with the Description of Four New Species, *Fieldiana Zoology* 2005: 1–53.

Velazco PM, Patterson BD. 2013. Diversification of the yellow-shouldered bats, genus *Sturnira* (Chiroptera, Phyllostomidae), in the New World tropics, *Molecular Phylogenetics and Evolution* 68: 683–698.

Velazco PM, Patterson BD. 2019. Small Mammals of the Mayo River Basin in Northern Peru, with the Description of a New Species of *Sturnira* (Chiroptera: Phyllostomidae), *Bulletin of the American Museum of Natural History* 2019: 1–70.

Wetterer AL, Rockman MV, Simmons NB. 2000. Phylogeny of Phyllostomid Bats (Mammalia: Chiroptera): Data from Diverse Morphological Systems, Sex Chromosomes, and Restriction Sites, *Bulletin of the American Museum of Natural History* 2000: 1–200.

Wiens JJ, Chippindale PT, Hillis DM. 2003. When are phylogenetic analyses misled by convergence? A case study in Texas cave salamanders, *Systematic Biology* 52: 501–514.

Xu H, Yuan Y, He Q, Wu Q, Yan, Q, Wang Q. 2012. Complete mitochondrial genome sequences of two Chiroptera species (*Rhinolophus luctus* and *Hipposideros armiger*), *Mitochondrial DNA* 23(4): 327–328.

Yoon KB, Kim JY, Cho JY, Park YC. 2011. The complete mitochondrial genome of the greater horseshoe bat subspecies, *Rhinolophus ferrumequinum korai* (Chiroptera: Rhinolophidae), *Mitochondrial DNA* 22(4): 102–104.

LIST OF TABLES

Table 1. List of specimens used in the present study. Records include taxonomic information, voucher identification, GenBank accession number, and bibliographic reference.

Table 2. Nucleotide data set used in this study. "Full outgroup dataset" corresponds to the complete sample of 71 sequences, "Reduced outgroup dataset" corresponds to a sub-sample made up of 48 sequences. The partition schemes are described and the Akaike Information Criterion values are compared. The asterisks (*) denote the best-evaluated partition schemes by this criterion.

Table 3. Amino acids data set used in this study. "Full outgroup dataset" corresponds to the complete sample of 71 sequences, "Reduced outgroup dataset" corresponds to a sub-sample made up of 48 sequences. The partition schemes are described and the Akaike Information Criterion values are compared. The asterisks (*) denote the best-evaluated partition schemes by this criterion.

Table 4. General features of the 32 new bat mitogenome assemblies.

SUPPLEMENTARY TABLE

Table S1. Taxonomic and collection data from Ecuadorian specimens analyzed in this study and whose mitogenome sequences were generated (see Table 1 for GenBank accession numbers). Altitude in meters above the see level. Weight in grams, standard external measures in mm. GPS coordinates in decimal degrees.

LIST OF FIGURES

Figure 1. Geographical distribution of specimens used in this work. Sampling localities: Pichincha: 1) Alambi (Lon: -78.680733, Lat: -0.030217); Santo Domingo de Los Tsáchilas: 2) Río Mulaute (Lon: -78.993183, Lat: -0.131917); 3) La Lorena (Lon: -79.139733, Lat: -0.2747998); 4) Hacienda Tinalandia (Lon: -79.054433, Lat: -0.2979668); 5) Reserva Otongachi (Lon: -78.9518828, Lat: -0.3212998); Cotopaxi: 6) Guasaganda (Lon: -79.1468667, Lat: -0.7798167); 7) Jardín de los Sueños (Lon: -79.2045668, Lat: -0.8372); 8) San Cristóbal (Lon: -79.1532668, Lat: -0.8607); 9) Manguilita El Triunfo (Lon: -79.20735, Lat: -0.9117498); Manabí: 10) Las Tunas (Lon: -80.8152861, Lat: -1.6621917)

Figure 2: Phylogeny of Phyllostomidae based on complete mitochondrial genomes (nucleotide sequences). The tree represents the best Maximum Likelihood phylogeny inferring Phyllostomidae and other chiropteran lineages' relationships. The tree was reconstructed in RAxML under the GTR+GAMMA+I model using the Full outgroup data set (71 taxa, 14,703 nucleotides). Color filled semicircles on the nodes indicate ML bootstrap support (percentage) and Bayesian posterior probabilities (see inserted caption). The absence of a semicircle on the node indicates that it was not recovered by ML or Bayesian inferences. Each Navajo's Rug shows if the specified node was retrieved (black square) or not (white square) in different analyses performed (see inserted caption).

LIST OF SUPPLEMENTARY FIGURES

Figure S1: Phylogeny of Phyllostomidae based on mitochondrial genomes (amino acid sequences). The tree represents the best Maximum Likelihood phylogeny inferring Phyllostomidae and other chiropteran lineages' relationships. The tree was reconstructed in RAxML under the mtMAM and mtREV +I+G+F models using the Full outgroup data set (71 taxa, 3,606 amino acids). Color filled semicircles on the nodes indicate ML bootstrap support (percentage) and Bayesian posterior probabilities (see inserted caption). The absence of a semicircle on the node indicates that it was not recovered by ML or Bayesian inferences. Each Navajo's Rug shows if the specified node was retrieved (black square) or not (white square) in different analyses performed (see inserted caption).

Figure S2: Phylogeny of Phyllostomidae based on the protein coding genes (CDS) from our full nucleotide data set using a 36-partition scheme. The tree was reconstructed in RAxML under the GTR+GAMMA+I model. Color filled semicircles on the nodes indicate ML bootstrap support (percentage; see inserted caption).

TABLES

Table 1. List of specimens used in the present study. Records include taxonomic information, voucher identification, GenBank accession number, and bibliographic reference.

Family	Subfamily	Species	Voucher[a]	Accession Number	Reference
Chiroptera					
Hipposideridae	–	*Hipposideros armiger*	–	NC_018540	Xu *et al.* 2012
Molossidae	Molossinae	*Molossus molossus*	QCAZ18284	ON357729	This study
Molossidae	Molossinae	*Molossus molossus*	QCAZ18287	pending	This study
Mormoopidae	–	*Pteronotus rubiginosus*	ISEM-V-2322	NC_022425	Botero-Castro *et al.* 2013
Mystacinidae	–	*Mystacina tuberculata*	–	NC_006925	Unpublished
Noctilionidae	–	*Noctilio leporinus*	ISEM-V-1890	KU743910	Botero-Castro *et al.* 2018
Phyllostomidae	Carollinae	*Carollia brevicauda*	QCAZ18221	pending	This study
Phyllostomidae	Carollinae	*Carollia castanea*	QCAZ18219	pending	This study
Phyllostomidae	Carollinae	*Carollia perspicillata*	MHNG1972-003	HG003309	Botero-Castro *et al.* 2013
Phyllostomidae	Carollinae	*Carollia brevicauda*	QCAZ18226	pending	This study
Phyllostomidae	Desmodontinae	*Desmodus rotundus*	EBRG-L-1874	HG003310	Botero-Castro *et al.* 2013
Phyllostomidae	Desmodontinae	*Desmodus rotundus*	QCAZ18371	pending	This study
Phyllostomidae	Desmodontinae	*Diaemus youngii*	MSB-56205	KU743906	Botero-Castro *et al.* 2018
Phyllostomidae	Desmodontinae	*Diphylla ecaudata*	MSB-211697	KU743911	Botero-Castro *et al.* 2018
Phyllostomidae	Glossophaginae	*Anoura caudifer*	ROM-113962	HG003307	Botero-Castro *et al.* 2013
Phyllostomidae	Glossophaginae	*Anoura cultrata*	QCAZ18217	ON310503	This study
Phyllostomidae	Glossophaginae	*Anoura geoffroyi*	QCAZ18218	ON310504	This study
Phyllostomidae	Glossophaginae	*Brachyphylla cavernicum*	ISEM-V-2350	NC_022421	Botero-Castro *et al.* 2013
Phyllostomidae	Glossophaginae	*Choeroniscus godmani*	QCAZ18233	ON357720	This study
Phyllostomidae	Glossophaginae	*Glossophaga soricina*	QCAZ18230	ON321893	This study
Phyllostomidae	Glyphonycterinae	*Glyphonycteris daviesi*	ROM-41125	KU743912	Botero-Castro *et al.* 2018
Phyllostomidae	Lonchophyllinae	*Hsunycteris thomasi*	ISEM-V-1646	KU743907	Botero-Castro *et al.* 2018
Phyllostomidae	Lonchophyllinae	*Lonchophylla concava*	QCAZ18274	ON357727	This study
Phyllostomidae	Lonchophyllinae	*Lonchophylla concava*	QCAZ18273	pending	This study
Phyllostomidae	Lonchophyllinae	*Lonchophylla robusta*	QCAZ18236	ON357721	This study

Phyllostomidae	Lonchorhininae	*Lonchorhina aurita*	MVZ-185587	KU743908	Botero-Castro *et al.* 2018
Phyllostomidae	Macrotinae	*Macrotus californicus*	MSB-140888	KU743909	Botero-Castro *et al.* 2018
Phyllostomidae	Micronycterinae	*Micronycteris hirsuta*	QCAZ18237	ON357722	This study
Phyllostomidae	Micronycterinae	*Micronycteris megalotis*	ISEM-V-2620	HF947304	Botero-Castro *et al.* 2013
Phyllostomidae	Micronycterinae	*Micronycteris megalotis*	QCAZ18280	ON357728	This study
Phyllostomidae	Phyllostominae	*Chrotopterus auritus*	AMNH-M-272843	KU743905	Botero-Castro *et al.* 2018
Phyllostomidae	Phyllostominae	*Lophostoma brasiliense*	QCAZ18085	ON310506	This study
Phyllostomidae	Phyllostominae	*Lophostoma silvicola*	MNHN2004-352	NC_022424	Botero-Castro *et al.* 2013
Phyllostomidae	Phyllostominae	*Phyllostomus discolor*	QCAZ18297	ON357733	This study
Phyllostomidae	Phyllostominae	*Tonatia maresi*	MNHN2004-376	NC_022428	Botero-Castro *et al.* 2013
Phyllostomidae	Phyllostominae	*Vampyrum spectrum*	EBRG-L-1896	NC_022429	Botero-Castro *et al.* 2013
Phyllostomidae	Rhinophyllinae	*Rhinophylla pumilio*	ISEM-V-1992	NC_022426	Botero-Castro *et al.* 2013
Phyllostomidae	Stenodermatinae	*Artibeus aequatorialis*	QCAZ18246	ON357726	This study
Phyllostomidae	Stenodermatinae	*Artibeus jamaincensis*	–	NC_002009	Pumo *et al.* 1998
Phyllostomidae	Stenodermatinae	*Artibeus literatus*	QCAZ18245	ON357725	This study
Phyllostomidae	Stenodermatinae	*Artibeus lituratus*	–	NC_016871	Meganathan *et al.* 2012
Phyllostomidae	Stenodermatinae	*Artibeus ravus*	QCAZ18228	ON321891	This study
Phyllostomidae	Stenodermatinae	*Chiroderma salvini*	QCAZ18227	ON321890	This study
Phyllostomidae	Stenodermatinae	*Enchisthenes hartii*	QCAZ18229	ON321892	This study
Phyllostomidae	Stenodermatinae	*Platyrrhinus matapalensis*	QCAZ18238	ON357723	This study
Phyllostomidae	Stenodermatinae	*Platyrrhinus nigellus*	QCAZ18299	ON357734	This study
Phyllostomidae	Stenodermatinae	*Sturnira bakeri*	QCAZ18306	ON357735	This study
Phyllostomidae	Stenodermatinae	*Sturnira ludovici*	QCAZ18312	ON357738	This study
Phyllostomidae	Stenodermatinae	*Sturnira luisi*	QCAZ18241	ON357724	This study
Phyllostomidae	Stenodermatinae	*Sturnira bakeri*	QCAZ18307	ON357736	This study
Phyllostomidae	Stenodermatinae	*Sturnira bakeri*	QCAZ18308	ON357737	This study
Phyllostomidae	Stenodermatinae	*Sturnira tildae*	ISEM-V-2412	NC_022427	Botero-Castro *et al.* 2013
Pteropodidae	–	*Pteropus dasymallus*	–	NC_002612	Nikaido *et al.* 2000
Pteropodidae	–	*Pteropus scapulatus*	–	NC_002619	Lin & Penny, 2001
Pteropodidae	–	*Rosetus aegyptiacus*	–	NC_007393	Unpublished
Rhinolophidae	Rhinolophinae	*Rhinolophus ferrumequinum*	–	NC_016191	Yoon *et al.* 2011
Rhinolophidae	Rhinolophinae	*Rhinolophus formosae*	–	NC_011304	Unpublished

Rhinolophidae	Rhinolophinae	*Rhinolophus luctus*	–	NC_018539	Xu *et al.* 2012
Rhinolophidae	Rhinolophinae	*Rhinolophus monoceros*	–	NC_005433	Lin *et al.* 2002
Rhinolophidae	Rhinolophinae	*Rhinolophus pumilus*	–	NC_005434	Nikaido *et al.* 2001
Vespertilionidae	Vespertilioninae	*Lasiurus borealis*	LSUMZ (field number CSM 020)	NC_016873	Meganathan *et al.* 2012
Vespertilionidae	Vespertilioninae	*Myotis albescens*	QCAZ18292	ON357731	This study
Vespertilionidae	Vespertilioninae	*Myotis formosus*	–	NC_015828	Kim *et al.* 2011
Vespertilionidae	Vespertilioninae	*Myotis riparius*	QCAZ18293	ON357732	This study
Vespertilionidae	Vespertilioninae	*Myotis riparius*	QCAZ18288	ON357730	This study
Vespertilionidae	Vespertilioninae	*Pipistrellus abramus*	–	NC_005436	Nikaido *et al.* 2001
Vespertilionidae	Vespertilioninae	*Plecotus auritus*	–	NC_015484	Unpublished
Vespertilionidae	Vespertilioninae	*Plecotus rafinesquii*	LSUMZ (field number M8121)	NC_016872	Meganathan *et al.* 2012
Vespertilionidae	–	*Chalinolobus tuberculatus*	–	NC_002626	Lin & Penny, 2001
Other mammals					
Bovidae	–	*Bos taurus*	–	NC_006853	Unpublished
Canidae	–	*Canis lupus*	–	NC_002008	Kim *et al.* 1998

[a] Key to institutional abbreviations: **AMNH** – American Museum of Natural History, New York, USA; **EBRG** – Museum "Estación Biológica de Rancho Grande", Aragua, Venezuela; **ISEM** – University of Montpellier, Montpellier, France; **LSUMZ** – Louisiana State University Museum of Natural Science, Baton Rouge, USA; **MHNG** – Natural History Museum of Geneva, Geneva, Switzerland; **MNHN** – Museum National d'Histoire Naturelle, Paris, France; **MSB** – Museum of Southwestern Biology, Albuquerque, USA; **MVZ** – Museum of Vertebrate Zoology at the University of California, Berkeley, USA; **QCAZ** – Zoology Museum, Pontifical Catholic University of Ecuador, Quito, Ecuador; **ROM** – Royal Ontario Museum, Toronto, Canada.

Table 2. Nucleotide data set used in this study. "Full outgroup dataset" corresponds to the complete sample of 71 sequences, "Reduced outgroup dataset" corresponds to a sub-sample made up of 48 sequences. The partition schemes are described and the Akaike Information Criterion values are compared. The asterisks (*) denote the best-evaluated partition schemes by this criterion.

	Bioinformatics software	Partition scheme	Number of partitions	Number of Parameters	-lnL	AIC
Full outgroup dataset	RAxML-NG	A single partition	1	149	-334,497.3	669,292.6
	RAxML-NG	rRNA + tRNA + protein-coding genes	14	292	-326,799.5	653,985.1
	RAxML-NG	rRNA + tRNA + codon positions	5	193	-332,165.0	664,914.0
	RAxML-NG	rRNA + tRNA + protein-coding genes + codon positions	38	556	-324,889.2	650,890.4*
	PartitionFinder RAxML-NG	Partition by gene	31	436	-330,755.8	662,383.7
	IQTREE2	Partition by gene	19	148	-339,430.8	679,157.6
Reduced outgroup dataset	RAxML-NG	A single partition	1	103	-219193.7	438,593.4
	RAxML-NG	rRNA + tRNA + protein-coding genes	14	246	-217376.1	435,244.2
	RAxML-NG	rRNA + tRNA + codon positions	5	147	-212155.9	424,605.8
	RAxML-NG	rRNA + tRNA + protein-coding genes + codon positions	38	510	-210734.2	422,488.4*
	PartitionFinder RAxML-NG	Partition by gene	28	358	-213561.8	427,839.7
	IQTREE2	Partition by gene	16	254	-211257.2	423,022.5

Table 3. Amino acids data set used in this study. "Full outgroup dataset" corresponds to the complete sample of 71 sequences, "Reduced outgroup dataset" corresponds to a sub-sample made up of 48 sequences. The partition schemes are described and the Akaike Information Criterion values are compared. The asterisks (*) denote the best-evaluated partition schemes by this criterion.

	Bioinformatic software	Partition scheme	Number of partitions	Number of Parameters	-lnL	AIC
Full outgroup dataset	RAxML-NG	A single partition	1	141	-75,293.4	150,868.7
	RAxML-NG	Protein-coding genes	12	231	-70,132.27	140,726.5
	PartitionFinder RAxML-NG	Partition by gene	7	178	-70,134.5	140,625.1*
	IQTREE2	Partition by gene	4	159	-73617.015	147,552.03
Reduced outgroup dataset	RAxML-NG	Partition by gene	1	95	-50,664.04	101,518.09
	RAxML-NG	Protein-coding genes	12	185	-46,991.45	94,352.90
	PartitionFinder RAxML-NG	Partition by gene	6	147	-46.976.63	94,247.27*
	IQTREE2	Partition by gene	4	113	-49,380.65	98,987.31

Table 4. General features of the 32 new bat mitogenome assemblies.

QCAZ	Species	Total reads[a]	Mean Coverage	mtDNA Reads	mtDNA Reads (%)	Mitogenome Length	G+C Content (%)[b]
18085	*Lophostoma brasiliense*	5,020,095	5,931	630,938	12.57	16,653	40.7
18217	*Anoura cultrata*	5,196,044	4,675	491,888	9.47	16,552	38.67
18218	*Anoura geofroyi*	5,387,000	4,910	513,801	9.54	16,605	39.87
18219	*Carollia castanea*	6,010,339	6,504	733,256	12.2	16,711	41.45
18221	*Carollia brevicauda*	714,6821	7,043	784,051	10.97	16,711	41.45
18226	*Carollia brevicauda*	7,153,480	6,414	770,227	10.77	16,711	41.45
18227	*Chiroderma salvini*	5,376,798	11,000	1,129,92	21.01	16,689	41.36
18228	*Artibeus ravus*	5,546,264	5,943	634,436	11.44	16,709	37.84
18229	*Enchisthenes hartii*	5,082,139	6,758	703,230	13.84	16,718	38.22
18230	*Glossophaga soricina*	5,389,214	3,055	347,814	6.45	16,529	37.35
18233	*Choeroniscus minor*	6,611,734	217	24,935	0.38	16,637	37.59
18236	*Lonchophylla robusta*	5,501,494	6,901	720,793	13.1	16,666	43.68
18237	*Micronycteris hirsuta*	5,244,058	10,723	1,109,69	21.16	16,589	42.85
18238	*Platyrrhinus matapalensis*	5,362,494	6,572	664,783	12.4	16,541	40.68
18241	*Sturnira bakeri*	5,818,828	6,939	787,240	13.53	16,637	43.27
18245	*Artibeus literatus*	4,412,371	943	104,092	2.36	16,709	37.84
18246	*Artibeus aequatorialis*	5,470,809	3,540	368,764	6.74	16,709	37.84
18273	*Lonchophylla concava*	4,421,729	2,306	232,980	5.27	16,691	39.65
18274	*Lonchophylla concava*	3,878,886	780	81,974	2.11	16,692	39.97
18280	*Micronycteris megalotis*	5,125,473	7,611	790,574	15.42	16,589	42.79
18284	*Molossus molossus*	4,834,631	3,731	385,460	7.97	16,612	36.26
18287	*Molossus molossus*	5,164,704	6,877	713,304	13.81	16,615	36.54
18288	*Myotis riparius*	5,610,421	8,940	994,147	17.72	17,052	35.57
18292	*Myotis albescens*	4,967,853	3,058	326,789	6.58	17,128	35.58
18293	*Myotis riparius*	4,441,706	2,722	318,278	7.17	17,186	35.81
18297	*Phyllostomus discolor*	4,216,226	3,482	359,346	8.52	16,692	41.74
18299	*Platyrrhinus nigellus*	5,369,804	5,302	553,748	10.31	16,541	40.68
18306	*Sturnira bakeri*	5,518,196	8,591	914,490	16.57	16,637	43.27
18307	*Sturnira bakeri*	5,365,597	9,504	995,712	18.56	16,637	43.27
18308	*Sturnira bakeri*	5,973,325	9,823	1,040,51	17.42	16,637	43.27
18312	*Sturnira ludovici*	4,528,183	8,222	864,316	19.09	16,646	43.61
18371	*Desmodus rotundus*	6,115,261	12,311	1,389,88	22.73	16,668	47.68

[a] trim / merge / duplicate
[b] Approximate values on draft genomes

Table S1. Taxonomic and collection data from Ecuadorian specimens analyzed in this study and whose mitogenome sequences were generated (see Table 1 for GenBank accession numbers). Altitude in meters above the sea level. Weight in grams, standard external measures in mm. GPS coordinates in decimal degrees.

Museum number	Field number	Genus	Species	Sex	Age	Province	Precise locality	Longitude	Latitude	Altitude	Weight	Forearm	Head-body length	Tail length	Ear length	Hind foot length
QCAZ18085	NK298731	*Lophostoma*	*brasiliense*	F	Adult	Santo Domingo de los Tsáchilas	La Lorena	-79.139733	-0.2747998	577	8	34	53.7	8	20.2	8.6
QCAZ18217	QKM54786	*Anoura*	*cultrata*	F	Adult	Cotopaxi	San Cristóbal	-79.1532668	-0.8607	517	18.5	41.9	53.7	-	10.8	10.3
QCAZ18218	QKM54793	*Anoura*	*geoffroyi*	M	Adult	Cotopaxi	Jardín de los sueños	-79.2045668	-0.8372	621	13	41.7	68.8	-	17.3	11.4
QCAZ18219	QKM54798	*Carollia*	*castanea*	M	Adult	Cotopaxi	San Cristóbal	-79.1532668	-0.8607	460	10.5	34.4	47.5	12	16.5	11
QCAZ18221	QKM54776	*Carollia*	*brevicauda*	M	Adult	Cotopaxi	Jardín de los sueños	-79.2045668	-0.8372	400	14.5	39.2	47.3	10.2	17.2	10.7
QCAZ18226	QKM54797	*Carollia*	*brevicauda*	F	Adult	Cotopaxi	San Cristóbal	-79.1532668	-0.8607	462	14	41.6	62	10.2	9	12
QCAZ18227	QKM54794	*Chiroderma*	*salvini*	F	Adult	Cotopaxi	Jardín de los sueños	-79.2045668	-0.8372	621	27	49.5	65.5	-	14.8	12.8
QCAZ18228	QKM54800	*Artibeus*	*ravus*	M	Subadult	Cotopaxi	Manguilita El Triunfo	-79.20735	-0.9117498	312	10.5	38.5	45.9	-	15.7	11
QCAZ18229	QKM54795	*Enchisthenes*	*hartii*	F	Adult	Cotopaxi	Jardín de los sueños	-79.2045668	-0.8372	573	18	40.5	51.3	-	15.4	9.3
QCAZ18230	QKM54777	*Glossophaga*	*soricina*	F	Adult	Cotopaxi	Jardín de los sueños	-79.2045668	-0.8372	395	9	35	44	5.4	13.1	9
QCAZ18233	QKM54807	*Choeroniscus*	*minor*	F	Adult	Cotopaxi	Jardín de los sueños	-79.2045668	-0.8372	495	8	35.1	41.4	5.5	10.5	9.3

QCAZ18236	QKM54804	*Lonchophylla*	*robusta*	M	Adult	Cotopaxi	Manguilita El Triunfo	-79.20735	-0.9117498	285	15	43.7	52.5	12.8	17	13.7
QCAZ18237	QKM54805	*Micronycteris*	*hirsuta*	F	Adult	Cotopaxi	Jardín de los sueños	-79.2045668	-0.8372	473	13.5	43.2	51	13.2	22.7	12.9
QCAZ18238	QKM54801	*Platyrrhinus*	*matapalensis*	M	Adult	Cotopaxi	Manguilita El Triunfo	-79.20735	-0.9117498	285	14	32.9	52.3	-	17	11.7
QCAZ18241	QKM54792	*Sturnira*	*luisi*	M	Adult	Cotopaxi	Guasaganda	-79.1468667	-0.7798167	481	21.5	41.8	56.6	-	15.9	10.8
QCAZ18245	NK298728	*Artibeus*	*literatus*	F	Adult	Santo Domingo de los Tsáchilas	La Lorena	-79.139733	-0.2747998	577	80	74.2	105.5	-	20.4	17.8
QCAZ18246	NK298686	*Artibeus*	*aequatorialis*	M	Adult	Santo Domingo de los Tsáchilas	Reserva Otongachi	-78.9518828	-0.3212998	856	46	65	89	-	22	14
QCAZ18273	NK298727	*Lonchophylla*	*concava*	F	Adult	Santo Domingo de los Tsáchilas	La Lorena	-79.139733	-0.2747998	577	6.5	33.2	56.9	9.5	11.5	8.2
QCAZ18274	NK298732	*Lonchophylla*	*concava*	F	Adult	Santo Domingo de los Tsáchilas	La Lorena	-79.139733	-0.2747998	577	7	34	58.6	11.3	14.4	10.4
QCAZ18280	NK298706	*Micronycteris*	*megalotis*	M	Adult	Santo Domingo de los Tsáchilas	La Lorena	-79.139733	-0.2747998	577	5.5	36	49	12	20	10
QCAZ18284	NK298713	*Molossus*	*molossus*	M	Adult	Santo Domingo de los Tsáchilas	La Lorena	-79.139733	-0.2747998	577	17	39	65	44	14	11
QCAZ18287	NK298712	*Molossus*	*molossus*	F	Adult	Santo Domingo de los Tsáchilas	La Lorena	-79.139733	-0.2747998	577	22	42	69	44	15	12
QCAZ18288	NK298683	*Myotis*	*riparius*	M	Adult	Santo Domingo de los Tsáchilas	Reserva Otongachi	-78.9518828	-0.3212998	856	4.5	35	46	35	14	7
QCAZ18292	NK298716	*Myotis*	*albescens*	F	Adult	Santo Domingo de los Tsáchilas	Río Mulaute	-78.993183	-0.131917	549	5	37	52	33	15	9
QCAZ18293	NK298651	*Myotis*	*riparius*	F	Adult	Pichincha	Alambi	-78.680733	-0.030217	1479	5	36	46	37	14	7

QCAZ18297	NK298644	*Phyllostomus*	*discolor*	M	Adult	Pichincha	Alambi	-78.680733	-0.030217	1496	45	64	94	10	24	19
QCAZ18299	NK298679	*Platyrrhinus*	*nigellus*	M	Adult	Pichincha	Alambi	-78.680733	-0.030217	1492	28.5	79	75	-	18	14
QCAZ18306	NK298688	*Sturnira*	*bakeri*	F	Adult	Santo Domingo de los Tsáchilas	Reserva Otongachi	-78.9518828	-0.3212998	856	14.5	42	61	-	16	13
QCAZ18307	NK298689	*Sturnira*	*bakeri*	M	Adult	Santo Domingo de los Tsáchilas	Reserva Otongachi	-78.9518828	-0.3212998	856	22	43	66	-	18	12
QCAZ18308	NK298692	*Sturnira*	*bakeri*	M	Adult	Santo Domingo de los Tsáchilas	Hacienda Tinalandia	-79.054433	-0.2979668	685	21.5	44	64	-	17	12
QCAZ18312	NK298640	*Sturnira*	*ludovici*	M	Adult	Pichincha	Alambi	-78.680733	-0.030217	1496	25	47	75	-	19	15
QCAZ18371	QKM54671	*Desmodus*	*rotundus*	F	Adult	Manabí	Las Tunas	-80.8152861	-1.6621917	11	36	60.5	68.8	-	20.3	15.6

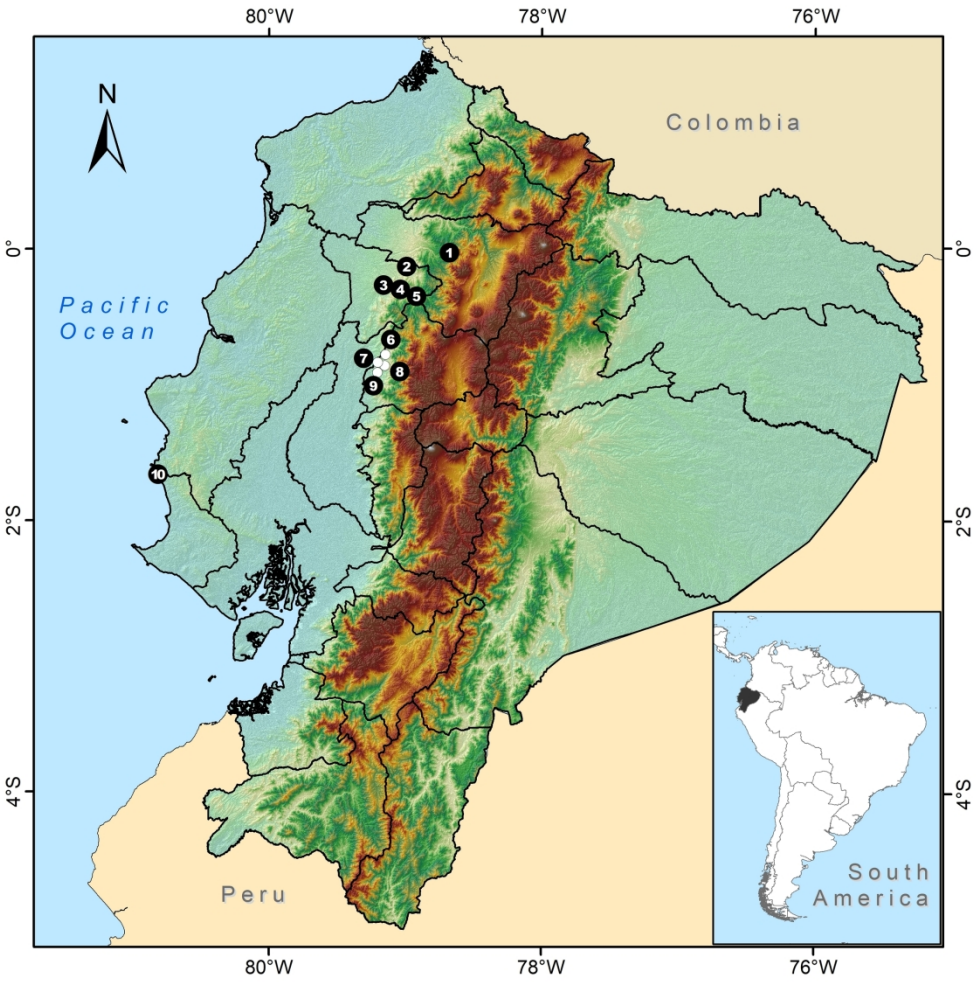

Figure 1. Geographical distribution of specimens used in this work. Sampling localities: Pichincha: 1) Alambi (Lon: -78.680733, Lat: -0.030217); Santo Domingo de Los Tsáchilas: 2) Río Mulaute (Lon: -78.993183, Lat: -0.131917); 3) La Lorena (Lon: -79.139733, Lat: -0.2747998); 4) Hacienda Tinalandia (Lon: -79.054433, Lat: -0.2979668); 5) Reserva Otongachi (Lon: -78.9518828, Lat: -0.3212998); Cotopaxi: 6) Guasaganda (Lon: -79.1468667, Lat: -0.7798167); 7) Jardín de los Sueños (Lon: -79.2045668, Lat: -0.8372); 8) San Cristóbal (Lon: -79.1532668, Lat: -0.8607); 9) Manguilita El Triunfo (Lon: -79.20735, Lat: -0.9117498); Manabí: 10) Las Tunas (Lon: -80.8152861, Lat: -1.6621917)

219x219mm (300 x 300 DPI)

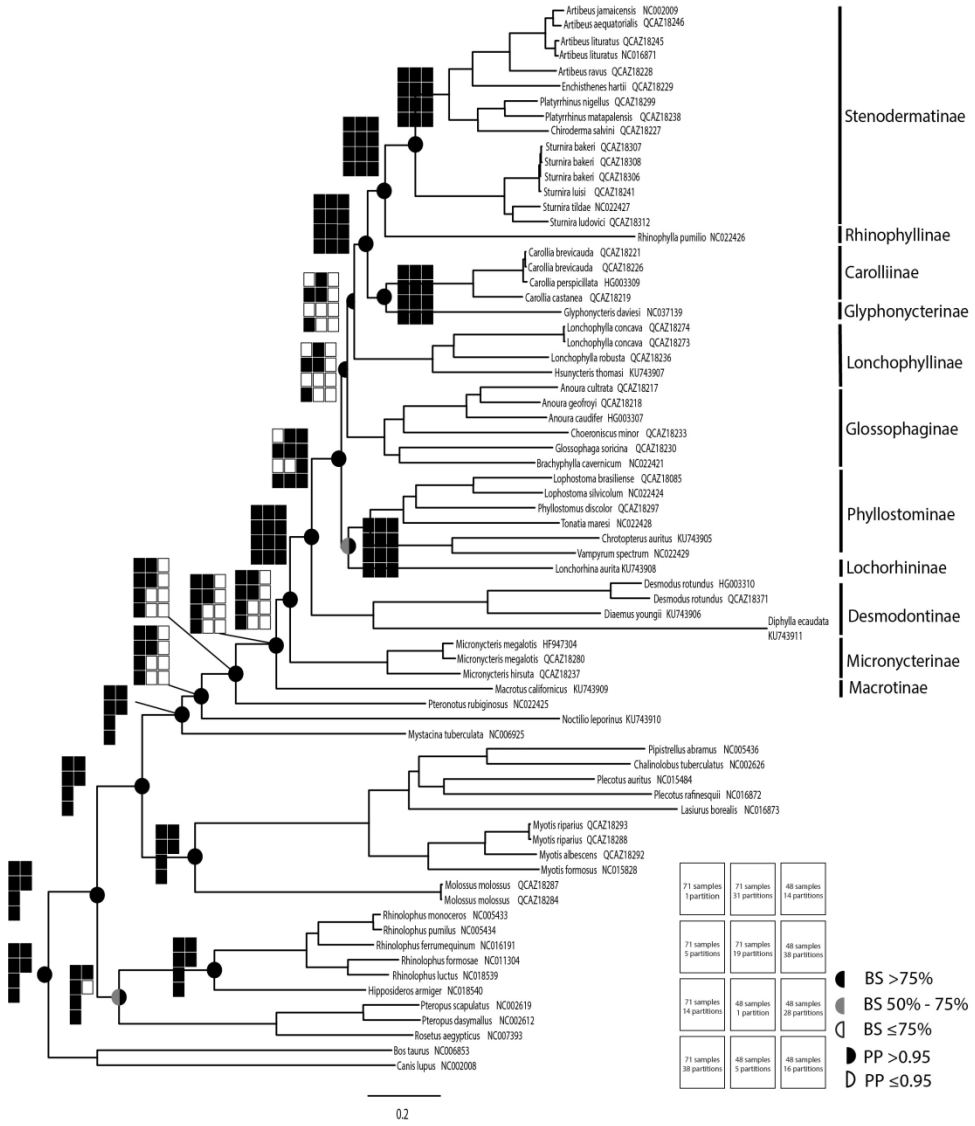

Figure 2: Phylogeny of Phyllostomidae based on complete mitochondrial genomes (nucleotide sequences). The tree represents the best Maximum Likelihood phylogeny inferring Phyllostomidae and other chiropteran lineages' relationships. The tree was reconstructed in RAxML under the GTR+GAMMA+I model using the Full outgroup data set (71 taxa, 14,703 nucleotides). Color filled semicircles on the nodes indicate ML bootstrap support (percentage) and Bayesian posterior probabilities (see inserted caption). The absence of a semicircle on the node indicates that it was not recovered by ML or Bayesian inferences. Each Navajo's Rug shows if the specified node was retrieved (black square) or not (white square) in different analyses performed (see inserted caption).

213x238mm (300 x 300 DPI)

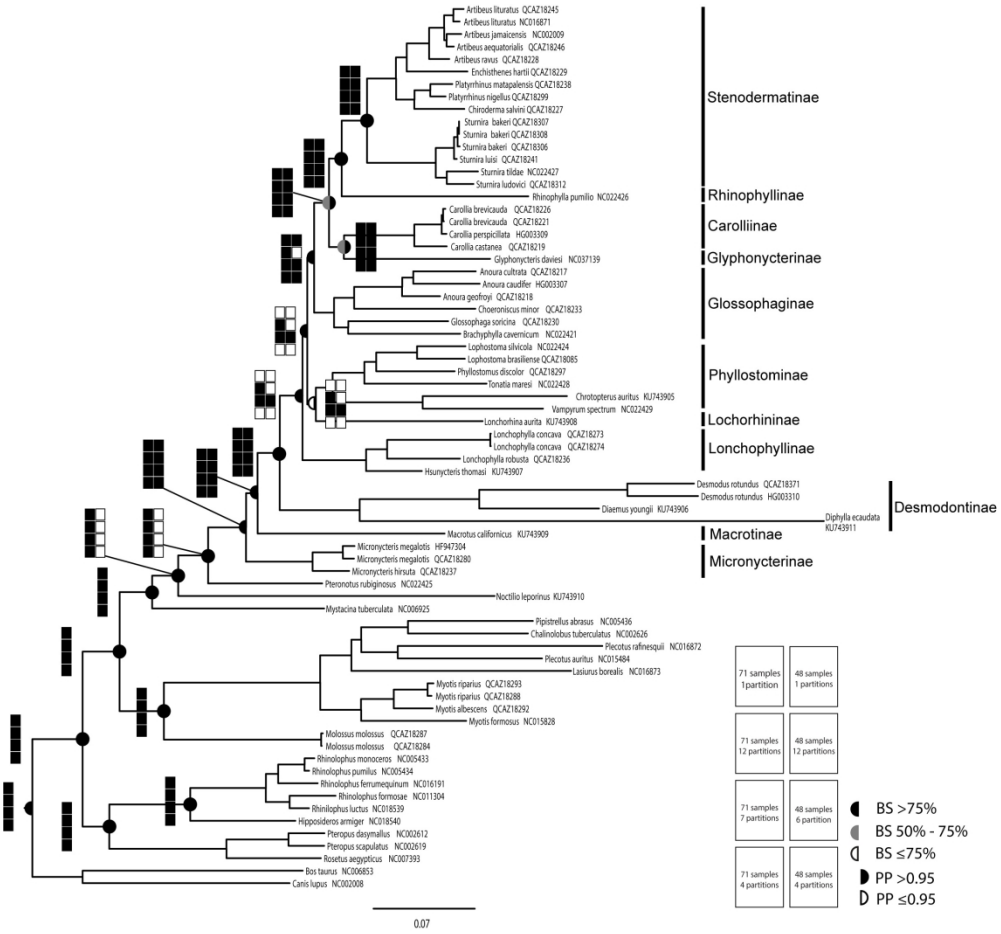

Figure S1: Phylogeny of Phyllostomidae based on mitochondrial genomes (amino acid sequences). The tree represents the best Maximum Likelihood phylogeny inferring Phyllostomidae and other chiropteran lineages' relationships. The tree was reconstructed in RAxML under the mtMAM and mtREV +I+G+F models using the Full outgroup data set (71 taxa, 3,606 amino acids). Color filled semicircles on the nodes indicate ML bootstrap support (percentage) and Bayesian posterior probabilities (see inserted caption). The absence of a semicircle on the node indicates that it was not recovered by ML or Bayesian inferences. Each Navajo's Rug shows if the specified node was retrieved (black square) or not (white square) in different analyses performed (see inserted caption).

207x192mm (300 x 300 DPI)

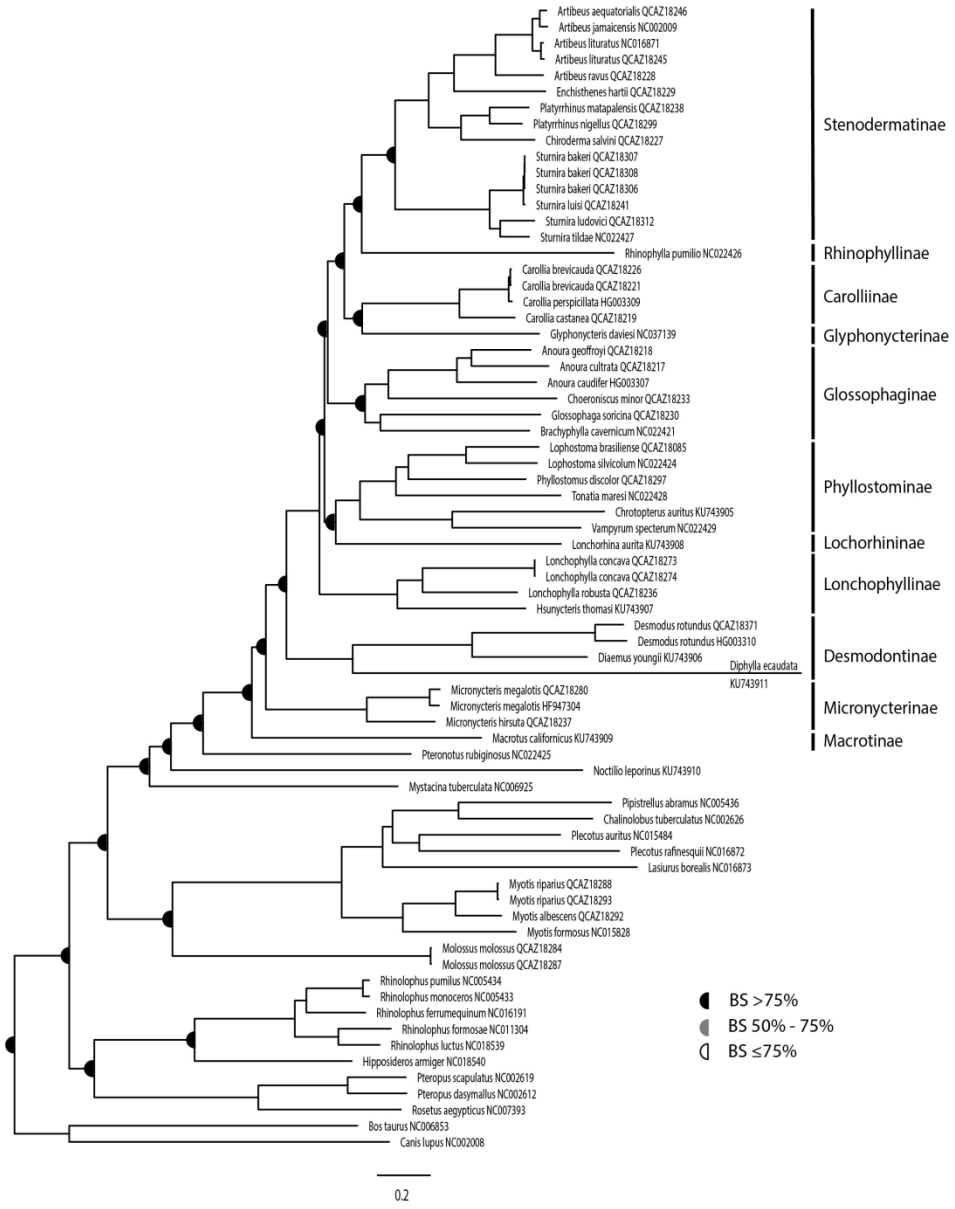

Figure S2: Phylogeny of Phyllostomidae based on the protein coding genes (CDS) from our full nucleotide data set using a 36-partition scheme. The tree was reconstructed in RAxML under the GTR+GAMMA+I model. Color filled semicircles on the nodes indicate ML bootstrap support (percentage; see inserted caption).

199x253mm (300 x 300 DPI)